Chemical Engineering Journal 468 (2023) 143589

Contents lists available at ScienceDirect

Chemical Engineering Journal

journal homepage: www.elsevier.com/locate/cej

An integrated Metagenomic-Pangenomic strategy revealed native microbes and magnetic biochar cooperation in plasticizer degradation

Mengyuan Ji [a], Ginevra Giangieri [a], Muhammad Usman [b], Chao Liu [c], Matteo Bosaro [d], Filippo Sessa [e], Paolo Canu [e], Laura Treu [a], Stefano Campanaro [a,*]

[a] Department of Biology, University of Padova, Via U. Bassi 58/b, 35121 Padova, Italy
[b] Department of Civil and Environmental Engineering, University of Alberta, Edmonton, AB T6G 2W2, Canada
[c] Guangdong Key Laboratory of Integrated Agro-Environmental Pollution Control and Management, Institute of Eco-environmental and Soil Sciences, Guangdong Academy of Sciences, Guangzhou 510650, China
[d] Italiana Biotecnologie, Via Vigazzolo 112, 36054 Montebello Vicentino, Italy
[e] Department of Industrial Engineering, University of Padova, Via Marzolo 9, 35131 Padova, Italy

ARTICLE INFO

Keywords:
Plasticizers
Magnetic biochar
Degradation
Metagenome
Pangenome

ABSTRACT

There has been growing concern over the release of plasticizers from plastic products, and the high levels of plasticizers in the environment have led to a threat to ecological security. Although some plasticizers may naturally degrade, their slow removal and prolonged life cycle remain challenges. To address this, this study explored a unique hybrid strategy using native field microorganisms and magnetic biochar (MBC) to support the upstream degradation of plasticizers. Diethyl phthalate (DP) was used as the test subject. The study found that MBC treatment led to high level of total organic carbon (TOC) and various organic products, demonstrating the degradation of DP. Analysis of the hybrid metagenomic model showed that several species of *Pseudomonas* can degrade downstream phenylmethanal and *Pseudomonas nitroreducens* has the ability to cooperate well with MBC due to its iron receptor and transporter. Additionally, a *Pigmentiphaga* species was found to have the ability to fully mineralize DP. Analysis of the *Pigmentiphaga* pangenome revealed that genes related to DP biodegradation were shared by members of this genus. Although some members of *Pseudomonas* is known to be pathogenic, the species identified in the study may not be harmful as they lack virulence factors. The study provides evidence regarding the cooperation between native biodegraders and MBC in mineralizing plasticizers, offering a new solution for removing phthalate plasticizers from soil and surface water.

1. Introduction

Phthalates (PAEs) are commonly utilized as plasticizers within the plastic industry to enhance the flexibility, transparency, durability, and lifespan of plastics [1]. However, these phthalate-based plasticizers have a tendency to leach into the environment rather than forming a covalent bond with the resin [2]. Due to their extensive use, plasticizer contaminants have been identified in various environments such as surface waters, sediments, agricultural fields, and soils located near industrial sites [3]. Hence, the development of a sustainable and efficient method to remove these pollutants is imperative as PAEs have a limited biodegradation rate [4].

The behavior of plasticizer pollutants is controlled by complex dynamic physical, chemical, and biological processes, including adsorption/desorption [5], leaching [6,7], chemical/biological degradation [8,9], plants uptake [10], and runoff [11]. However, these traditional methods are not without risks and limitations. Potential concerns include ineffectiveness for certain pollutants, recontamination, mobilization, generation of harmful byproducts, and persistence in the environment [12,13]. In contrast, microbial degradation provides a sustainable and eco-friendly approach to soil remediation that effectively treats a broad range of pollutants without generating harmful

Abbreviations: MBC, Magnetic biochar; DP, Diethyl phthalate; TOC, Total organic carbon; PA, Phenylmethanal; PAEs, Phthalates; EEM, Excitation-emission matrix; GC–MS, Gas chromatography-mass; BC, Biochar; SP, Sodium persulfate; AOPs, Advanced oxidation process; DOM, Dissolved organic matter; PARAFAC, Parallel Factor; EI, Electron impact; MAGs, Metagenome assembled genomes; RPKM, Reads per kilobase million; ARGs, Antibiotic resistance genes; Ex, Excitation; Em, Emission; envMAGs, MAGs obtained from environmental.

* Corresponding author.
E-mail address: stefano.campanaro@unipd.it (S. Campanaro).

https://doi.org/10.1016/j.cej.2023.143589
Received 21 March 2023; Received in revised form 13 May 2023; Accepted 15 May 2023
Available online 18 May 2023

byproducts or emissions [14]. However, the potential for release and degradation as well as microbial responses to PAEs in farmland-water systems are not well understood, yet. Although various studies have focused on the potential of natural microorganisms to digest PAEs [15,16], the microbial degradation of PAEs in environments often takes a long time and requires specific conditions favoring microbial growth and acclimatization [17]. For instance, a 35 days-long experiment revealed that native soil microorganisms alone were unable to reduce dioctyl phthalate concentrations by more than 20% [18]. Another investigation revealed that di-n-octyl phthalate degraded slowly even when bioaugmentation was made using adaptive activated sludge [19]. However, a recent investigation found that a combination of oxidation processes and stressors significantly accelerated the biodegradation of bis(2-ethylhexyl) phthalate decreasing the degradation time to just 24 days [20]. This highlights the crucial role of external stimulation in enhancing the degradation of plasticizer pollutants known as PAEs. The distinct nature of paddy soil, characterized by frequent flooding, creates favorable conditions for various chemical reactions, making it important to conduct further research on the degradation potential of PAEs in this type of farmland-water system. A more detailed investigation of this environment will provide relevant information that will help in mitigating the negative impacts of these pollutants.

Biochar (BC)-based multifunctional materials have gained widespread recognition for their environmental friendliness, efficiency, and ability to remediate contaminated soils [21,22]. One particular type of biochar-based material, Magnetic Biochar (MBC), is formed through the pyrolysis activation or chemical co-precipitation of transition metals such as Fe, Co, and Ni with the biochar substrate [23]. These transition metals on MBC can help activate free radicals in the environment, such as sulfate radicals, to selectively degrade recalcitrant pollutants like PAEs [20]. BC has the ability to indirectly stimulate microorganisms by providing a favorable habitat within its porous structure, and its nutrient absorption capacity can continuously support microbial growth [24], thereby enabling certain microorganisms to synergistically remove pollutants with BC. Despite the potential benefits of MBC in degrading PAEs, there has been limited research on the degradation potential obtained through the interaction between MBC and native microbes in response to external stimulation. While some studies have focused on changes in soil microbial communities in the presence of PAEs, few have investigated the functional responses of specific microbial species. As a result, it remains unclear which microorganisms are responsible for PAE degradation in farmland-water systems and how MBC-microbe interactions play a role in the degradation of PAEs. Further investigation is needed to fully understand these interactions and the potential of biochar-based materials in remediation efforts.

The current study aims to investigate the collaborative degradation of plasticizers in flooded soil using MBC and naturally occurring field microorganisms. Diethyl phthalate (DP) was selected as the model PAEs for this investigation since it is one of the most widely utilized PAEs in comparison to other plasticizer types and has been found in numerous contaminated fields [25]. A multidisciplinary approach was employed to characterize the metabolic processes involved in DP degradation. This approach involved identifying the organic levels and components present in contaminated soil leachate and DP released in the aqueous environment. Total organic carbon (TOC) analyzer, excitation-emission matrix (EEM) fluorescence spectroscopy, and gas chromatography-mass (GC–MS) spectrometry were combined to analyze the samples. In addition, high-precision Illumina short-reads and large-span nanopore long-reads were used together to obtain detailed information on the microbial communities present in the complex farmland soil–water system. Putative MBC cooperating species and microbes with the ability to autonomously degrade DP were obtained, and their potential pathways for metabolizing DP were investigated. Pangenomic evidence suggests that related members of the *Pigmentiphaga* genus share the ability to degrade DP, and we further investigated these species for their potential antibiotic resistance and pathogenicity in the environment.

2. Materials and methods

2.1. Preparation of biochar and chemicals

The preparation of biochar and magnetic biochar was conducted using rice straw as the raw material. Rice straw was subjected to drying, crushing, and sieving with a 60-mesh sieve prior to use. A portion of the treated rice straw was then mixed with urea, ascorbic acid, and $FeSO_4{\cdot}7H_2O$, placed in an autoclave, sealed, and subjected to a heating process at 160 °C for 10 h. After the mixed material was taken out and dried for 24 h, it was subjected to pyrolysis in a tube furnace at the temperature of 700 °C under N_2 gas for 2 h. The solid material obtained after pyrolysis was then taken out. The solid material that has undergone mixed liquid pretreatment was named MBC, and the material obtained by pyrolysis of the original rice straw was named BC. Fig. S1 presents the surface structure and elemental composition of the magnetic biochar. The diethyl phthalate (C_6H_4-1,2-$(CO_2C_2H_5)_2$, ≥99%), Sodium persulfate (SP, $Na_2S_2O_8$, ≥ 99.5%), urea (NH_2CONH_2, 99%), and ascorbic acid used in the experiment were purchased from Sigma-Aldrich.

2.2. Release experiment in water

To explore the potential and characteristics of DP dissolution in water under different conditions, a release experiment was conducted. DP was dissolved in ultra-high quality Milli-Q water by adding 0.45 mL DP to 80 mL of water in a 120 mL amber glass bottle, and the mixture was shaken at 150 rpm for 24 h to evaluate the release properties. A separate set of experiments was performed to assess the impact of MBC on the DP aqueous solution. In these experiments, 0.5 g of MBC and 2.25 mmol of sodium persulfate (SP) were added to the DP aqueous solution. The contact time was maintained at 24 h, and dissolved organic matter samples were collected through a 0.45 μm membrane filter and stored at −20 °C for further analysis.

2.3. Microcosm incubations and sampling

Soil samples were collected from a depth of 2–20 cm in a paddy field located in Grumolo delle Abbadesse (VI, Italy) (45°30′36.8″N 11°39′29.3″E). The samples were dried, ground, and sieved through a 40-mesh sieve for later use. A microcosm incubation experiment was conducted with three replicates for each of the following treatments: Control, BC and DP, MBC and DP, and DP-contaminated treatment. The experimental setup involved filling 120 mL serum bottles with 50 g of soil and 80 mL of sterile ultrapure water. Then, 2.25 mmol DP were added to the microcosm to achieve of 1% (w/w) ratio of the dry weight of soil. The advanced oxidation process (AOPs) was then triggered by adding SP to the MBCDP treatment (SP were added according to the DP ratio of 1:1). The microcosms were incubated in the dark at 25 °C and wrapped in aluminum foil to prevent evaporation.

After the first week of incubation, the liquid phase was collected, and the collection was repeated every two weeks thereafter. The liquid phase was sampled with a 2 mL syringe, centrifuged at 4000 rpm (Eppendorf 5804R centrifuge) for 10 min, and the upper liquid layer was stored at −20 °C for the subsequent analysis of dissolved organic matter (DOM). After the long-term incubation, the mixture in the microcosm was subjected to high-speed centrifugation for 10 min at 4000 rpm (Eppendorf 5804R centrifuge). The obtained liquid samples were stored at −20 °C for later determination of organic matter.

2.4. Methodology for integrated liquid analysis

The TOC content of liquid samples was measured using high-temperature catalytic combustion to CO_2 on a TOC analyzer (TOC-L CPH, Shimadzu, Japan). The instrument was calibrated with potassium hydrogen phthalate. Prior to analysis, the liquid samples were filtered through 0.45 μm filters to remove any particulate matter.

The structural properties of the liquid samples were characterized using EEM fluorescence spectroscopy (Aqualog; Horiba-Jobin Yvon, USA). Using MATLAB Version 8.5.0197613 for Parallel Factor (PARAFAC) modeling as previously described [26].The instrument had an excitation range of 240 to 600 nm and an emission range of 280 to 550 nm. To correct for Rayleigh scattering, the raw EEM data was normalized. The fluorescence spectra of Milli-Q water was taken under the same conditions to control for the effects of Raman scattering.

Organic components of the liquid samples were analyzed using GC–MS (Clarus® 580, Clarus® SQ 8, USA). The instrument was operated in full scan mode (m/z 50–350), with electron impact (EI) mode at 70 eV and an ion source temperature of 220 °C. The temperature program for the GC oven started at 40 °C, held for 2 min, then ramped up to 280 °C at a rate of 10 °C/min and held for 9 min. Helium was used as the carrier gas. Chemical identification was based on comparison of the obtained mass spectra to the NIST mass spectral database [27]. Details regarding the samples preparation for GC–MS are available in the Supporting Information.

2.5. DNA extraction and sequencing

After long-term incubation, collect the homogenized soil mixture from each microcosm for microbialanalysis. DNA was extracted from the soil slurry using DNeasy PowerSoil® (QIAGEN GmbH, Hilden, Germany) with minor modifications according to the protocol of manufacturer. NanoDrop (ThermoFisher Scientific, Waltham, MA) and Qubit fluorometer (Life Technologies, Carlsbad, CA) were used to check the quantity and quality of extracted samples. Shotgun sequencing was performed using the Illumina NovaSeq platform at the Sequencing Facility of the DPartment of Biology, University of Padova. Total DNA from all samples was pooled and used to build a long-read library with the Rapid Barcoding kit (SQK-RBK004). A FLO-MIN106 R9 flow cell on a MinION device was then used to sequence the long-read library (Oxford Nanopore Technologies, Oxford, UK).

2.6. Hybrid assembly and genomic data analysis

Sequence data were deposited at the Sequence Read Archive (SRA, NCBI) under Bioproject PRJNA892267. The process of hybrid assembly, binning, functional annotation, and classification of metagenome assembled genomes (MAGs), as well as the calculation of reads per kilobase million (RPKM) per sample, are thoroughly described in the Supporting Information.

Additional genomes/MAGs associated with putative DP degraders were downloaded from the NCBI database and used for pangenome analysis. Genome was assessed for completeness and contamination using Checkm2 [28] and subsequently annotated individually for each metagenome following the above protocol. The maximum-likelihood trees were generated with fasttree2 [29] using the binary presence and absence of accessory genes, and were visualized in phandango [30]. Antibiotic resistance genes (ARGs) were annotated using the Comprehensive Antibiotic Research Database [31]. Predict the bacterial virulence of selected MAGs using the VFanalyzer [32].

2.7. Statistical

The two-sided Welch's t-test was used to determine the significance of differences in the number of genes associated to different functional categories in MAGs. Difference in the number of genes belonging to different categories were also estimated considering treatments and blank. Based on statistical results from the Fisher exact test, the "annotate" and "enrichment" functions of the EnrichM (v0.6.30) were used to identify enzymes enriched in MAGs associated to particular treatments (https://github.com/geronimp/enrichM).

3. Results and discussion

3.1. Liquid phase organic properties of different treatments

The effect of AOPs activated by MBC on DP in a water environment was evaluated through a release experiment. Figure S1 illustrates the successful loading of Fe and N onto the surface of the prepared MBC. Previous research has shown that Fe-N co-doped BC has the ability to activate PS through a series of free-radical and non-free-radical pathways, resulting in the production of highly oxidizing free radicals such as •OH, $\bullet SO_4^-$, and $^1O_2$ that are capable of attacking and breaking the chemical bonds of pollutants [33]. Fig. 1 shows the organic structure properties and composition of the DP and MBCDP treatments after 24 h of shaking release. The excitation and emission (Ex/Em) peak at 275/340 nm excited by DP is consistent with the position of tryptophan and protein-like substances, and the application of MBC significantly reduced the fluorescence intensity at this position. It has been reported in the literature [34] that the fluorescence intensity of furans and organic acids can be significantly lower compared to phenolic aromatic compounds. The use of MBC in this study resulted in a decrease in fluorescence intensity, which is believed to be caused by the formation of degradation products like acetic acid, besides, the presence of redox reactions may also lead to fluorescence quenching in DOM [35]. The GC–MS analysis showed clearly that the peak area of DP (16.32 min) after treatment with MBC was significantly reduced by 52% (Fig. 1b). The released products were identified as Phenylmethanal (PA) (7.34 min) and benzylic alcohol (8.56 min). The high peak value of PA revealed a successful attack on the single bonds "C-C" and "C-O", as well as the double bond "C = O" of DP.

Fig. 2 presents the organic properties of the soil leachate obtained from the long-term incubation experiment. The changes in the TOC of soil leachate among different treatments during the incubation period are depicted in Fig. 2a. Initially, no significant differences were observed among the DP, BCDP, and MBCDP treatments. However, a marked decrease in TOC was observed in the BCDP treatment after 21 days of incubation and it remained similar to the blank group in the later stages, while the TOC of the DP and MBCDP groups increased over time, reaching 4270 mg/kg soil and 3480 mg/kg soil respectively on the 49th day. The observation that the BCDP group showed low TOC values is consistent with previous reports of efficient DP adsorption by biochar soil composites [36,37]. The elevated TOC in the MBCDP treatment indicated that adsorption is no longer the dominant mechanism, and that the buildup of intermediate products could contribute to the increase in TOC content. It can be inferred that MBC, which has a similar porous structure to BC, is capable of adsorbing and aggregating organic pollutants. The aggregation of DP on the surface of MBC makes it more susceptible to attack by free radicals such as $\bullet SO_4^-$ generated by AOPs. Additionally, studies have shown that the oxygen-containing functional groups of MBC promote the generation of $\bullet SO_4^-$ in the Fe_3O_4/PS system [38], enhancing the attack efficiency on organic matter and leading to the accumulation of more intermediate products. This warrants further experimental validation in the future. The increase in TOC in soil solely contaminated with DP can be attributed to the high solubility of DP in water (1080 mg/L at 25 °C) [39], which resulted in its gradual integration into the soil leachate over time.

EEM equipped with PARAFAC identified four principal components with distinct Ex/Em (Fig. 2b, Table1). Component 1 (C1) evidenced two prominent EX/Em peaks at 250 nm and 425 nm, as well as at 325 nm and 425 nm. This spectral pattern aligns with the characteristics of substances similar to humic acids. Prior studies have established the widespread presence of C1 in rice soil [40]. Component 2 (C2) displayed a maximum EX/Em peak at 275 nm/340 nm and is related to substances similar to tryptophan and proteins [41]. Furthermore, its spectral position matches that of the excitation spectrum of DP solvent. Component 3 (C3) exhibited a peak position at 250 nm/500 nm, which is indicative of anthropogenic UVA humic or fulvic acid substances originating from

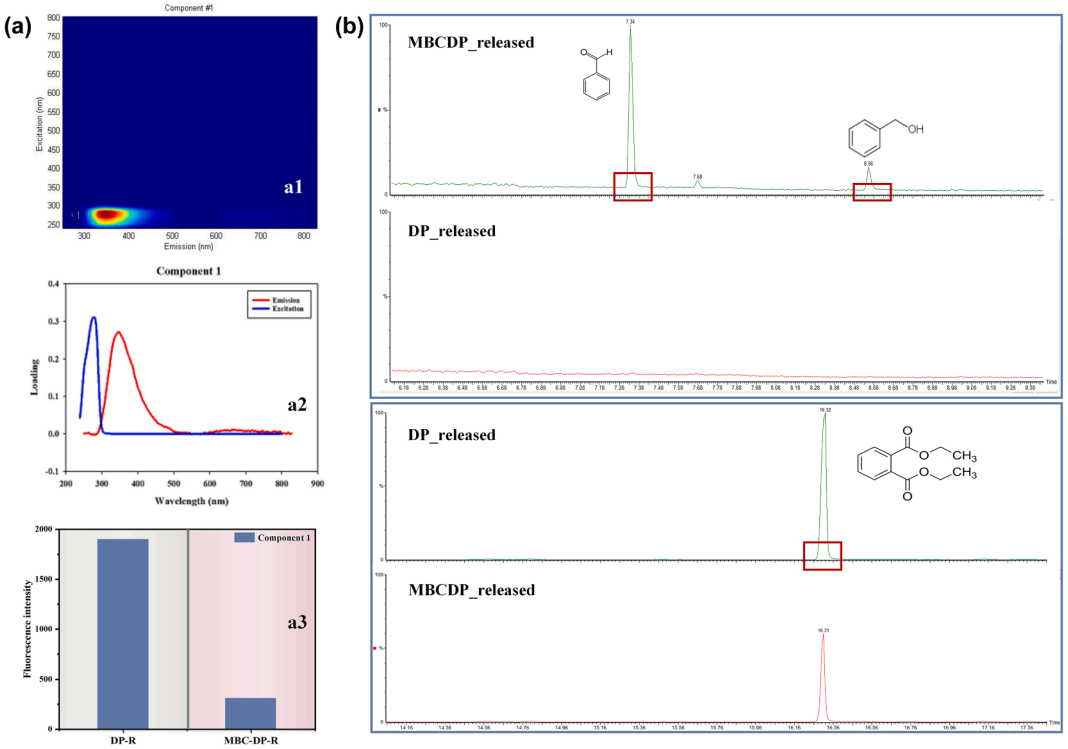

Fig. 1. The properties of organic matter obtained from the oscillatory release experiments of DP and MBCDP treatments. (a) Fluorescence properties of released substances identified by EEM spectroscopy. The fluorescence spectrum excited by DP in aqueous solution is referred to as a1, the corresponding excitation/emission wavelength is designated as a2, and the fluorescence intensity resulting from DP and MBCDP aqueous solution is represented by a3. (b) Organic compounds identified in DP and MBCDP aqueous solutions via GC–MS analysis.

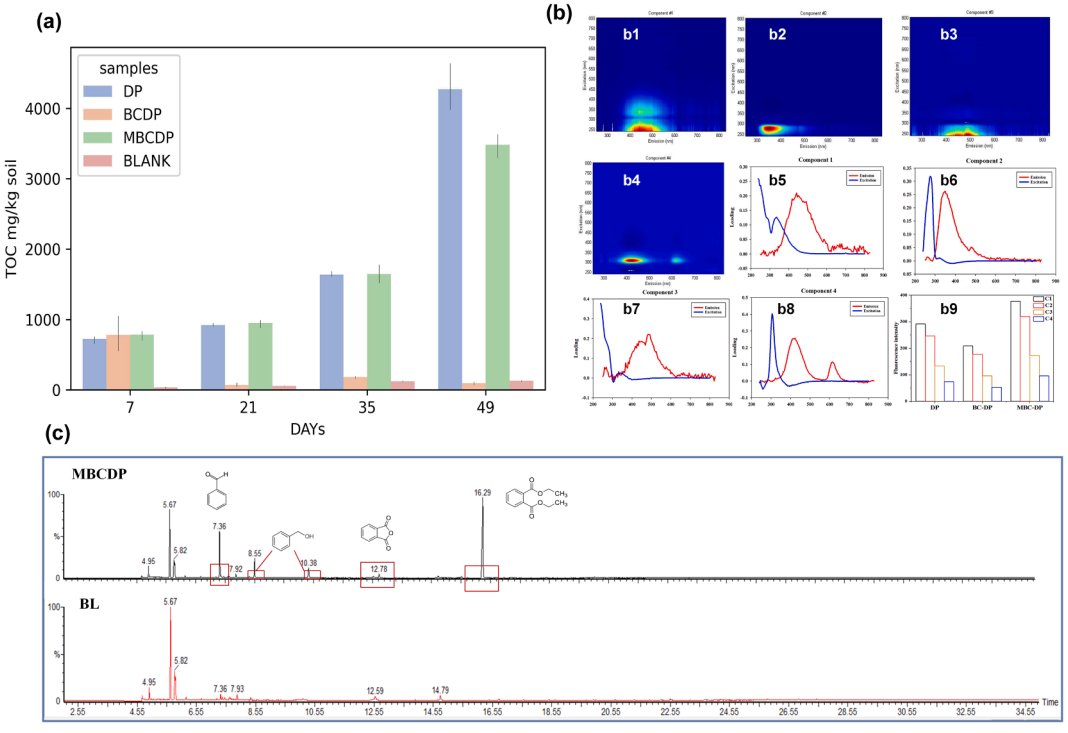

Fig. 2. Shifts in liquid phase. (a) Total organic carbon levels of soil solution from different treatments. (b) Structural features of liquid organic matter identified by EEM spectroscopy. The fluorescence spectrums excited by DOM in soil leachate are referred to as b1-4, the corresponding excitation and emission wavelengths are designated as b5-8, and the fluorescence intensity of the identified components among different treatments is denoted as b9. (c) Organic components in the liquid phase of MBCDP treatment identified by GC–MS spectroscopy.

Table 1
The fluorescent components of the DOM samples.

Components	Ex/Em(nm)	Description	Source
C1	250,325/425	Humic acid-like	Autochthonous
C2	275/340	tryptophan-like, protein-like	Autochthonous
C3	250/500	UVA humic-like	fulvic acid, terrestrial, autochthonous
C4	310/410,610	UVA marine humic-like	anthropogenic from wastewater and agriculture

terrestrial systems [42]. Component 4 (C4) displayed two emission peaks at (310, 410) nm and (310, 610) nm, which are attributed to UVA marine humic substances of anthropogenic origin from wastewater and agriculture [43]. This component was also in agreement with the fluorescence peak position of benzaldehyde, 4-hydroxy-3,5-dimethoxy, as reported in a previous study [34]. The distinct emission peak at 610 nm suggests the presence of higher molecular weight aromatic compounds [44]. These results showed that the fluorescence intensity of each component in the MBCDP treatment was significantly higher than that of the other two treatments. Although the TOC value of the DP treatment was higher than that of the MBCDP treatment, the fluorescence intensity of the fluorescent substances was lower in the DP treatment compared to the MBCDP treatment. The observed difference in soil organic matter may be attributed to a variety of factors, including redox reactions, condensation, concentration, and changes in ion exchange. For example, the polymerization and condensation of soil organic matter has been shown to lead to an increase in humic and fulvic acids [45]. Fenton oxidation has also been found to enhance the fluorescence intensity of aromatic functional groups in DOM by increasing the production of non-aromatic compounds and inorganic residues from proteins or humic substances [46]. Furthermore, the increase in C3 and C4 may be related to the accumulation of degradation products of DP in MBC treatment.

Soil leachate is known to have a complex composition that hinders the detection of high molecular weight compounds and limits the ability to directly quantify the products due to low concentrations of various organic compounds. To overcome these limitations, the samples were concentrated through evaporative drying and analyzed by GC–MS to provide qualitative evidence of liquid phase components (Fig. 2c). Despite the difficulties in detecting high-intensity peaks, the MBCDP treatment still produced distinct peaks for benzyl alcohol, phthalic anhydride, and diethyl phthalate. The larger peak area for PA at 7.36 min also indicated an increase in the content of benzaldehyde. In short, the presence of these components is in agreement with the results of the release experiment, providing direct evidence that the AOPs in the flooded soil environment were also successfully activated by elements of the MBC load, resulting in the attack of free radicals on DP and the accumulation of intermediate products such as PA.

3.2. Taxonomic composition of the microbiome in different treatments

Both a “global assembly analysis” and a “genome-centric metagenomic” approach were used to ascertain the role of the microbiome in various microcosm bottles. The former was based on gene finding and annotation on the entire assembly obtained from the combined assembly of Illumina and nanopore reads. The scaffolds underwent a binning process to identify the microbial genomes. This process allowed to recover 193 MAGs (completeness $\geq$ 50% and contamination $\leq$ 10%). 74 MAGs with a relative abundance greater than 1% were taxonomically assigned to 9 bacterial phyla, as depicted in Fig. 3. *Proteobacteria,* with 38 MAGs, dominated the microbial community and have been reported

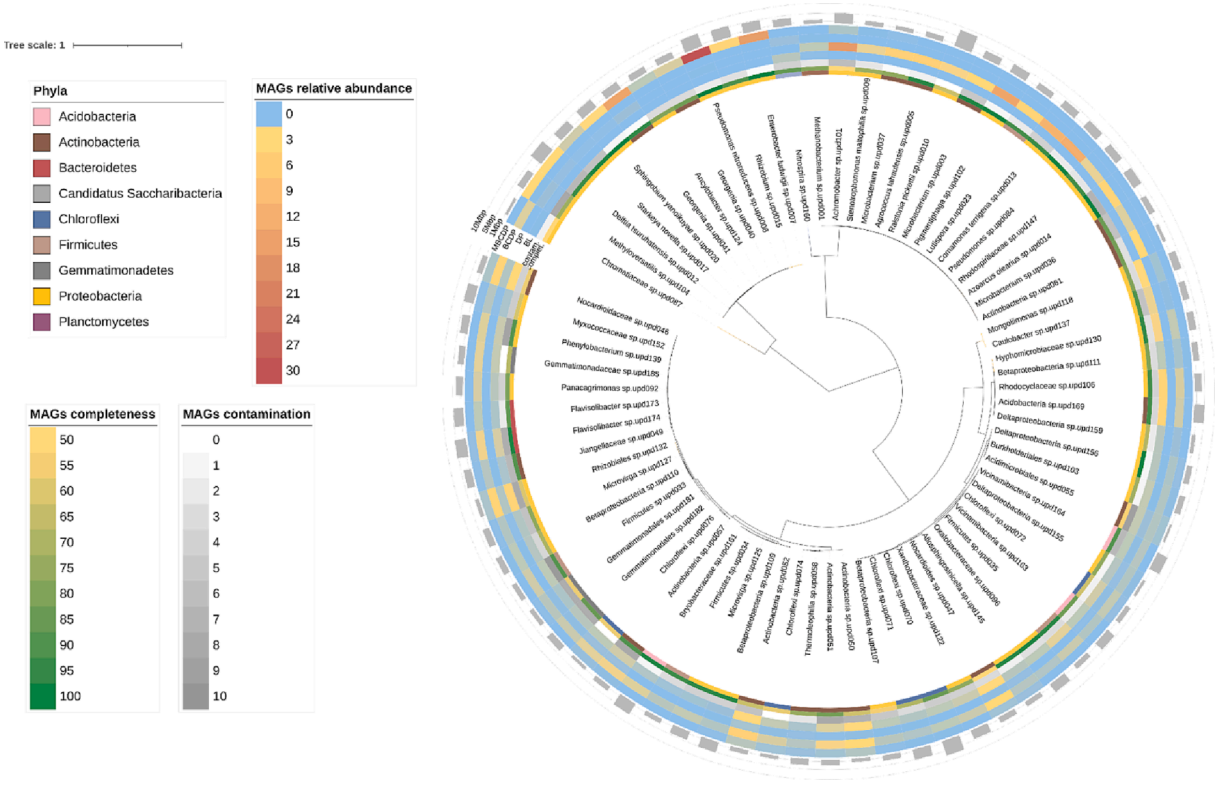

Fig. 3. Properties of 74 MAGs identified in the microbiome with relative abundance higher than 1%: MAG coverage, quality (completeness and contamination), and taxonomic assignment.

to play important roles in global nutrient cycling and carbohydrate metabolism [47]. The increased relative abundance of this phylum (37.5% in MBCDP and 32.2% in DP treatment compared to the blank) suggested an elevated level of carbohydrate metabolism in both treatments. *Firmicutes* (4 MAGs), previously reported to play key roles in lignocellulosic decomposition [48], showed a significant decrease in relative abundance in MBCDP treatment, suggesting that soil natural organic matter is not the main degradant of this group. Other phyla such as *Gemmatimonadetes* (3MAGs), *Chloroflexi* (5MAGs), *Bacteroidetes* (2MAGs), and *Acidobacteria* (3MAGs) were significantly reduced in both DP and MBCDP treatments, while the relative abundance of *Actinobacteria* (17 MAGs) remained unchanged among the various treatments. These phyla have diverse metabolic pathways which are relevant for important biogeochemical cycles, decomposition of biopolymers, and secretion of exopolysaccharides [49–51]. The addition of DP may have altered the organic substrate levels of the paddy soil, affecting the abundance of these phyla.

Some specific MAGs belonging to the aforementioned phyla showed significant enrichment in response to different conditions. For instance, *Pseudomonas nitroreducens* sp. upd006 was found to have a relative abundance of up to 37.6% in the MBCDP group. Previous studies have linked this species with the degradation of aromatic compounds, including simazine and nicosulfuron [52]. Additionally, some of the highly abundant MAGs in the MBCDP treatment, such as *Georgenia* sp. upd041, *Rhizobium* sp. upd015, and *Methyloversatilis* sp. upd104, have been reported to be associated with the degradation of phthalic acid esters by soil bacterial communities [53,54]. This enrichment further supports the changes in microbial community composition observed as a result of the degradation of DP. The treatment of DP contamination also resulted in the significant enrichment of *Achromobacter* sp. upd101, *Pigmentiphaga* sp. upd102, *Pseudomonas* sp. upd084, and *Comamonas terrigena* sp. upd013. These microorganisms have the potential of utilizing DP as a direct carbon source for their growth. Nevertheless, microbial composition analysis alone provides limited information, and the evidence presented in later sections, based on genome-centric functional analysis, provides a more comprehensive and convincing assessment.

The variation in microbial community composition among the different treatments was illustrated through principal component analysis (PCA) (Figure S4). As depicted, the microbial composition in the BCDP treatment was similar to the Blank group, while the DP and MBCDP treatments were noticeably distinct from the control. This is in line with the observed changes in species relative abundance. The potential obligate or facultative nutritional modes of the microbiome members across the different treatments were further explored through a co-occurrence analysis (Figure S5). Fig. S5(b) depicts the co-occurrence network of several highly abundant MAGs that exhibit significant correlation (r greater than 0.5) (considering only the top 50 abundant MAGs). Notably, a significant positive association (r greater than 0.5, $P < 0.05$) was observed between *Pseudomonas nitroreducens* sp. upd006 and several MAGs, including *Georgenia* sp. upd041, *Rhizobium* sp. upd015, *Delftia tsuruhatensis* sp. upd012, *Sphingobium yanoikuyae* sp. upd020, and *Enterobacter ludwigii* sp. upd007. It has been reported that under simulated shallow aquifer conditions, *Sphingobium yanoikuyae* can convert DP to phthalic acid through successive hydrolysis or demethylation pathways [55]. Additionally, *Georgia*, *Ancylobacter*, and *Rhizobium* have been widely recognized for their ability to degrade polycyclic aromatic and xenobiotic organic pollutants [56–58]. This further suggests the possibility of complementary functional roles among these MAGs in response to the MBCDP treatment.

3.3. Functional prediction at the global level

Examining enzyme abundance among treatments can provide a clear understanding of how microbial communities contribute to the degradation of contaminants. The degradation of DP can be divided into two processes: upstream degradation (DP demethylation to form phthalic acid) and downstream degradation (phthalic acid mineralization). In this study, the RPKM values of genes in all samples were calculated and used as a proxi to assess the impact of different treatments on the upstream and downstream degradation of DP.

Fig. 4a compares the changes in abundance levels (calculated as RPKM values) of enzymes involved in the biodegradation process among different treatments. It is evident that the DP treatment had significantly higher levels of genes encoding phthalate transporter (ophD), phthalate 4,5-*cis*-dihydrodiol dehydrogenase (EC 1.3.1.64), phthalate 4,5-dioxygenase (EC 1.14.12.7), and phthalate 4,5-dioxygenase reductase component (EC:1.18.1.-) compared to the other treatments (Fig. 4A). Studies have shown that dioxygenase of Gram-negative bacteria first catalyze the formation of *cis*-4,5-dihydro-4,5-dihydroxyphthalate, followed by oxidation to 4,5-dihydroxyphthalate through NAD-dependent dehydrogenase [59]. Meanwhile, Gram-positive bacteria first oxidize PAEs to 3,4-dihydro-3,4-dihydroxyphthalate, which is deelectronized and dehydrogenated to produce 3,4-dihydroxyphthalate, followed by dehydrodecarboxylation [60]. Therefore, it is evident that the biodegradation process, which was controlled by gram-negative bacteria, dominated the DP treatment. In contrast, the levels of genes involved in the upstream degradation of DP in the MBCDP treatment were not significantly different from the blank sample. This suggests that the high organic matter levels in the MBCDP group did not result from direct degradation of DP by microorganisms. Further analysis was conducted to investigate the changes in genes encoding downstream benzoate metabolism among the treatments. It was observed that the MBCDP treatment showed higher levels of the gene encoding benzoate 1,2-dioxygenase (EC 1.14.12.10) compared to the other treatments, suggesting that the MBCDP group utilized MBC to directly achieve the upstream degradation of DP and relied on soil microorganisms for the cooperative mineralization of downstream PA.

The phylogenetic origins of DP degradation genes were explored by taxonomic classification of phthalate 4,5-dioxygenase (EC 1.14.12.7) and phthalate 4,5-dioxygenase reductase component (EC 1.18.1.-) genes, which control the first step in phthalate degradation (Fig. 4b). A total of 41 MAGs were found to contain genes encoding the enzymes EC 1.14.12.7 and EC 1.18.1.-. Among them, several species including *Pseudomonas nitroreducens* upd006, *Pigmentiphaga* sp. upd102, *Pseudomonas* sp. upd084, *Azoarcus olearius* sp. upd014, and *Methyloversatilis* sp. upd104, exhibited high gene copy numbers of these two enzymes (Fig. 4B). The distribution of these MAGs among different treatments is further displayed in Figure S6. It is clear that *Pseudomonas nitroreducens* sp. upd006, *Pseudomonas* sp. upd084 and *Pigmentiphaga* sp. upd102 not only exhibited high gene copy numbers of critical enzymes, but also were significantly enriched in the DP treatment or MBCDP treatment. This further qualifies them as potential DP degraders or possibly as species cooperating in MBC degradation.

The discovery of *Pigmentiphaga* sp. upd102, a microaerophilic, aromatic compound-degrading bacterium found exclusively in the DP treatment, is of significance. Previous studies have shown that species belonging to the genus *Pigmentiphaga* are capable of metabolizing aromatic compounds [61,62], and in this study *Pigmentiphaga* sp. upd102 showed a direct degradation potential for DP, therefore, it could represent a new DP degrader existing in natural paddy soil. To provide more logical and convincing proof of how these several MAGs contribute to the degradation of DP in different treatments, we further reconstructed the metabolic pathways of these MAGs and carried out comparative gene analysis.

3.4. Putative degradation pathways identified from metabolic reconstruction

3.4.1. Pseudomonas nitroreducens sp. upd006 and Pseudomonas sp. upd084

In this study, the species *Pseudomonas nitroreducens* sp. upd006 and *Pseudomonas* sp. upd084 were identified as being enriched in the

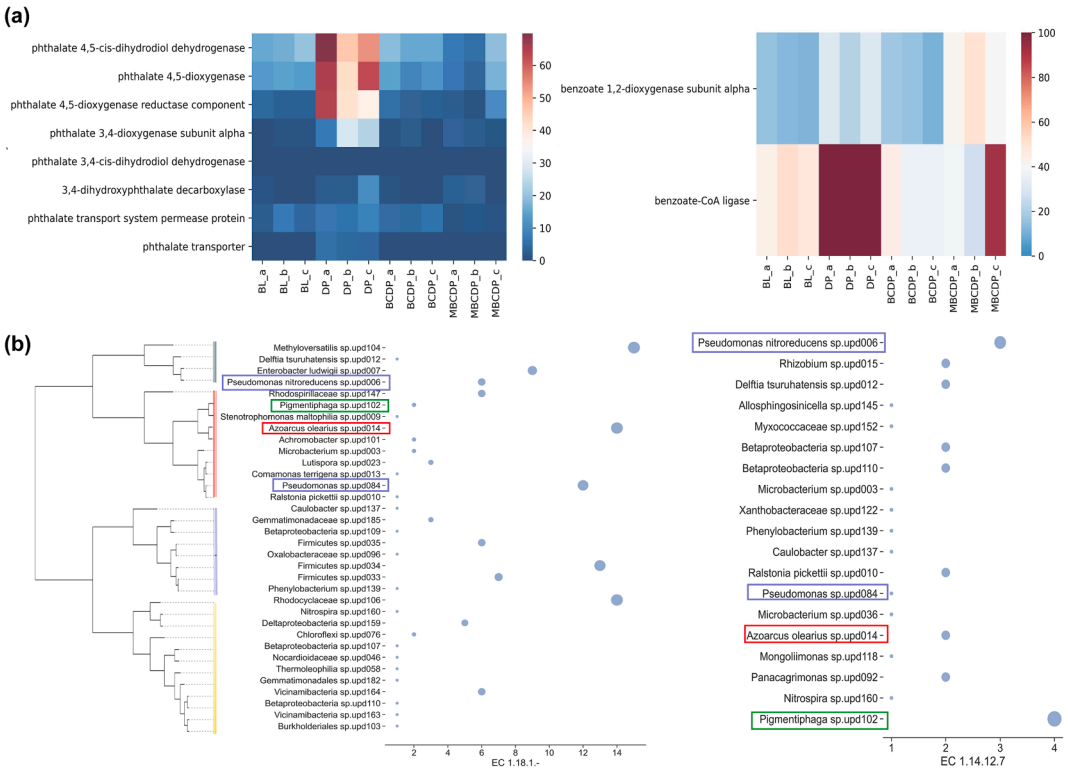

Fig. 4. Microbial functional activities potentially associated with DP degradation at the global level. (a) RPKM values of selected DP degrading enzymes among different treatments. RPKM values of all genes are reported in Table S2. (b) Gene copy numbers of phthalate 4,5-dioxygenase in MAGs.

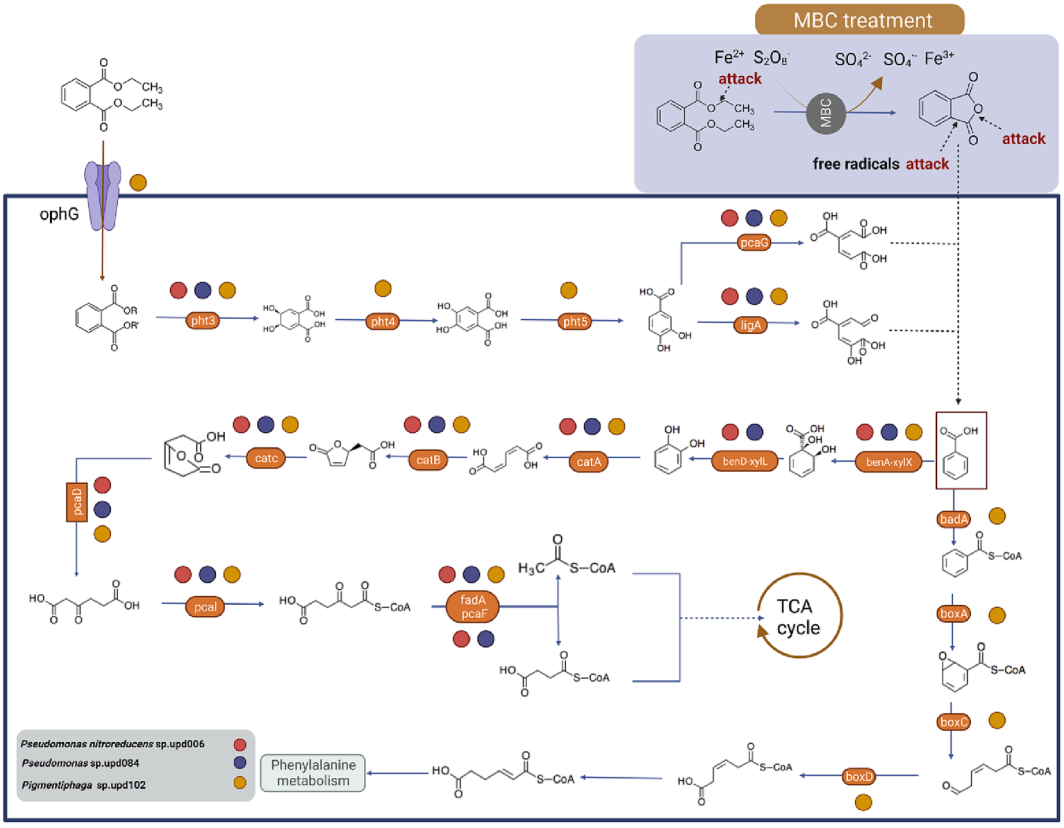

Fig. 5. Graphical representation of the proposed DP metabolic pathway based on three key species. The red, purple and yellow dots represent genes present in *Pseudomonas nitroreducens* sp. upd006, *Pseudomonas* sp. upd084, and *Pigmentiphaga* sp. upd102, respectively. All relevant genes considered for metabolic reconstruction can be found in Table S5. (For interpretation of the references to colour in this figure legend, the reader is referred to the web version of this article.)

MBCDP and DP groups, respectively. Previous research has indicated that members of the genus *Pseudomonas* have a role in the degradation of various phthalic lipids, such as dibutyl phthalate [63]. To gain further insight into the metabolic potential of these two MAGs, metabolic reconstructions were performed on their genomes, as depicted in Fig. 5. The red and purple dots indicate the annotated genes in *Pseudomonas nitroreducens* sp. upd006 and *Pseudomonas* sp. upd084, respectively. Our results indicated that although both *Pseudomonas nitroreducens* sp. upd006 and *Pseudomonas* sp. upd084 contain the gene encoding the phthalate 4,5-dioxygenase (pht3), they are lacking other essential genes in the upstream biodegradation pathway of DP and the transporter genes for PAEs (oph cluster). Despite the lack of these genes can be attributed to the incomplete genome reconstruction, this finding suggests that they cannot directly convert DP into PA. However, the downstream degradation pathway from PA is complete in both MAGs. PA was converted to catechol through the action of benzoate 1,2-dioxygenase and dihydroxycyclohexadiene carboxylate dehydrogenase, followed by a series of oxidases, isomerases, lipases, and transferases. This ultimately results in the production of Succinyl-CoA or Acetyl-CoA, which entered the tricarboxylic acid cycle.

The results obtained from the MBCDP treatment indicate a high prevalence of *Pseudomonas nitroreducens* sp. *upd006* in the samples. This suggests that this species is likely to be highly enriched with PA as a carbon source, particularly after intermediate PA is produced through oxidation. GC–MS analysis (Fig. 2C) supports the finding that firstly the C-O bond of DP is degraded to form phthalic anhydride, which was then further broken down to PA, and metabolized by *Pseudomonas nitroreducens* sp. upd006. The enrichment of *Pseudomonas* sp. *upd084* in the DP group appears to be linked to a mutualistic co-culture of microorganisms. As demonstrated in Figure S3, *Pseudomonas* sp. *upd084* exhibited a significant positive correlation with several MAGs that possess degradative potential. This suggests that the species may be able to metabolize intermediates produced by other species. In consideration of the functional similarity of *Pseudomonas nitroreducens* sp. upd006 and *Pseudomonas* sp. upd084 in the benzoate metabolism pathway, we conducted a comparative analysis of their gene content. The results of the comparison showed a high level of homology between the two MAGs (Figure S7).

The ability of *Pseudomonas* species to uptake and metabolize iron has been well documented [64]. In our study, both *Pseudomonas nitroreducens* sp. upd006 and *Pseudomonas* sp. upd084 possess complete polycyclic aromatic hydrocarbon degradation pathways. However, only *Pseudomonas nitroreducens* sp. upd006 was observed to be significantly enriched in the MBCDP group. This disparity between the two MAGs could be associated with the presence of ferrous iron (Fe(II)) and ferric iron (Fe(III)) in the reaction system activated by MBC. The Feo system is widely recognized as the primary ferrous (Fe(II)) transport system in prokaryotes [65]. FeoB, a large integral membrane protein, is believed to function as a ferrous permease, while FeoA can directly bind to FeoB. This FeoA-FeoB interaction is essential for the uptake of Fe(II) [66]. Our results, as anticipated, indicated the presence of genes encoding FeoA and FeoB in *Pseudomonas nitroreducens* sp. upd006 and their absence in *Pseudomonas* sp. upd084 (Table S3).

Furthermore, to postulate how the conversion process of Fe(II) to free ferric iron (Fe(III)) is working upon activation of the AOPs, we conducted an investigation into the related functional genes involved in Fe(III) recognition and transport in these two MAGs. The outer membrane TonB-dependent receptor and transporter FpvA and FptA, known for their high selectivity and affinity for Fe(III) [67], were only present in *Pseudomonas nitroreducens* sp. upd006 and absent in *Pseudomonas* sp. upd084. To assess the similarity of the Fe(II) and Fe(III) uptake and transport functions among members of the *Pseudomonas nitroreductase* species, a pangenome analysis was conducted (Table S4). The results showed that genes encoding ferrous (Fe(II)) transport were present in all of the analyzed MAGs/genomes, with the exception of one downloaded genome named *P. nitroreducens_contig1* having low completeness (87.57%), and the majority of them contained FpvA and FptA. These findings highlight the exceptional potential of *Pseudomonas nitroreducens* as a cooperative partner in MBC, with its ability to absorb both Fe(II) and Fe(III) generated during AOPs, while degrading upstream accumulated PA. In short, DP was initially attacked by free radicals activated by MBC in this soil–water environment, causing chemical bond cleavage as well as the release of iron elements. Co-occurring microorganisms such as *Sphingobium yanoikuyae* sp. upd020 and *Rhizobium* sp. upd015 may help mineralize DP and other intermediate products, leading to a significant accumulation of PA, which serves as a substrate for *Pseudomonas nitroreducens* sp. upd006. Furthermore, Fe(II) and Fe(III) in the process were absorbed by *Pseudomonas nitroreducens* sp. upd006, achieving harmless recycle of resources while mineralizing DP. This MBC-functional microbial combined system thus holds great promise for future biotechnological applications.

3.4.2. *Pigmentiphaga sp. upd102*

The yellow dots in Fig. 5 depict the genes annotated in *Pigmentiphaga* sp. upd102, whose whole-genome information is presented in Figure S8. Our analysis revealed the presence of a complete DP metabolic pathway in this MAG. The transport of PAEs into the bacterial cell is a critical metabolic step, which is facilitated by either the ABC transporter-type PAE transport system or, alternatively, by the permease-type PAE transporter [68]. In *Pigmentiphaga* sp. upd102, the phthalate transport protein (ophG) mediates the entry of DP into the cell, which is then converted into protocatechuate via the pht gene cluster. Finally, the protocatechuate undergoes degradation through protocatechuate dioxygenase to enter the benzoate degradation process. Compared to *Pseudomonas nitroreducens* sp. upd006 and *Pseudomonas* sp. upd084, *Pigmentiphaga* sp. upd102 exhibits a novel PA degradation pathway, converting PA to Benzoyl-CoA through benzoate-CoA ligase, ultimately generating 2,3-Didehydroadipyl-CoA which can enter the phenylalanine metabolism. The complete metabolic pathway of 2,3-Didehydroadipyl-CoA in *Pigmentiphaga* sp. upd102 is presented in the reconstructed phenylalanine metabolism map shown in Figure S9.

The degradation of DP by the genus *Pigmentiphaga* has not been previously reported. In order to determine the presence of DP degradation capability within the genus, a pangenome investigation was conducted utilizing information from *Pigmentiphaga*-related genomes/MAGs obtained from environmental (envMAGs) samples in the NCBI database (Table S6). The completeness of these envMAGs and *Pigmentiphaga* sp. upd102 varied between 73% and 100%, and the degree of contamination varied between 0% and 4.5%. In contrast, *Pigmentiphaga* sp. upd102 had low sequence homology to other *Pigmentiphaga* genomes/MAGs retrieved in the NCBI database. We further retrieved the annotations of the core gene clusters involved in phthalate metabolism in the *Pigmentiphaga* genomes (Fig. 6B). The gene *pht5* encoding 4,5-dihydroxyphthalate decarboxylase and terephthalate 1,2-dioxygenase oxygenase component (*tphA3*) were detected in all envMAGs and *Pigmentiphaga* sp. upd102. The complete pathway for converting phthalate to protocatechuate, as encoded by genes pht3-5, was observed in all MAGs except Pigmentiphaga sp. landfill_2 (73% completeness). Additionally, multiple envMAGs have genes (*ophG*, *ophH*) encoding PAE transporters, which may facilitate directly incorporating DP into the cell cytoplasm. Therefore, our putative DP mineralization pathway may be a ubiquitous capability in *Pigmentiphaga* based on evidence provided by the MAGs/genomes belonging to this genus.

3.5. *Antibiotic resistance and virulence factor of putative DP-degrading species*

The widespread presence of microplastics has raised concerns about the dissemination of antibiotic resistance genes (ARGs) [69] and pathogenic organisms [70]. The impact of chemical additives in plastics on the proliferation of ARGs and virulence factors is currently unclear. Hence, it is important to examine whether microbes performing DP

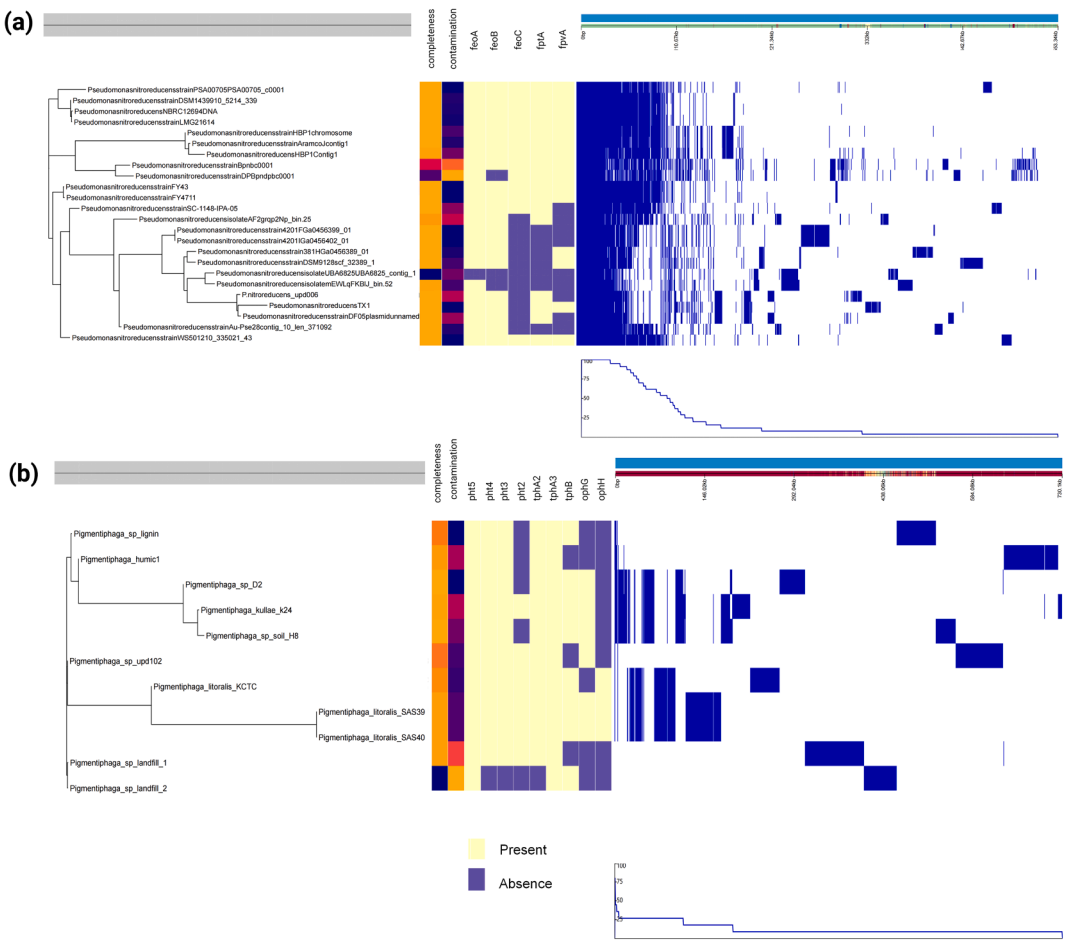

Fig. 6. Pangenome analysis of (a) *Pseudomonas nitroreducens* sp. upd006 and (b) *Pigmentiphaga* sp. upd102. All MAGs/genomes were retrieved from the NCBI database. The maximum-likelihood tree is generated using the binary presence and absence of accessory genes.

degradation contain ARGs and virulence factors, as this could impact their applicability in biodegradation of plasticizers.

All these three MAGs derived from the Pseudomonadota phylum contain ARGs that are linked to the resistance to specific types of drugs (Table S7). The most frequently occurring ARGs found in *Pigmentiphaga* sp. upd102 were those related to fluoroquinolone and tetracycline resistance. Similarly, both the two MAGs from the *Pseudomonas* genus showed strict hits for resistance to fluoroquinolone and tetracycline, as well as aminocoumarins, diaminopyrimidines, and phenols. Additionally, *Pseudomonas* sp. upd084 showed high hits for genes associated with resistance to benzalkonium chloride antibiotics. A more diverse set of ARGs was found in *Pseudomonas nitroreducens* sp. upd006, including those related to macrolide monobactam, carbapenem, cephalosporin, penam, peptide, sulfonamide, glycylcycline, and acridine dye resistance. These findings align with previous studies [71,72] and suggest that these three MAGs has the potential of spreading antibiotic resistance in the environment.

The existence of bacterial virulence factors can hinder the applicability of bacteria for engineering/bioremediation purposes, as they enable pathogenic bacteria to replicate and disseminate within a host by circumventing host defenses [73]. Our analysis identified multiple virulence factor-associated genes in three MAGs (Table S8). These included genes involved in amino acid and purine metabolism, biofilm formation, efflux pumps, and antiphagocytosis. Furthermore, genes related to Type IV pili biosynthesis, a key component of primary epithelial cell adhesion [74], were present in *Pseudomonas nitroreducens* sp. upd006 and *Pseudomonas* sp. upd084. The presence of known harmful virulence gene clusters in *Pseudomonas*, such as exotoxin A and metallophores [75,76], were not identified in the selected MAGs. In particular, the gene related to phytotoxin phaseolotoxin (*cysC1*) was detected in *Pseudomonas nitroreducens* sp. upd006. Although several virulence factors were identified, many of them serve essential metabolic functions necessary for bacterial survival, thus, it is conceivable that the potential DP degraders proposed in this work won't be pathogenic, making them suitable for use in the remediation of plasticizers in paddy soils and field runoff. However, the possible negative impact of *Pseudomonas nitroreducens* sp. upd006 on some plants should be noted.

4. Conclusion

Human activities have resulted in the influx of plastic waste into agricultural fields, leading to the accumulation of plastic additives in these environments. While the traditional methods of microbial degradation can be sluggish, incorporating magnetic biochar to activate the peroxidation process offers a promising avenue for facilitating the in-situ degradation of plasticizers. Indeed, this study demonstrated that hybrid magnetic biochar and field microorganisms, such as *Pseudomonas nitroreducens* sp. *upd006* that can uptake Fe(II) and Fe(III), were capable of mineralizing DP plasticizer. Additionally, the species *Pigmentiphaga* sp. upd102 was observed to have the potential of completely metabolize plasticizers in contaminated soil. A pangenome analysis also suggested that plasticizer mineralization may be a common trait among members of the *Pigmentiphaga* genus. The absence of pathogenicity virulence factors in the proposed potentially degrading or MBC-cooperating species makes them a promising option for removing plasticizers from surface water and farmland soils. However, to ensure the safe and

effective application of MBC in environmental remediation, it is crucial to consider how to design MBC to control its own toxicity and the environmental risks associated with free radicals.

Declaration of Competing Interest

The authors declare that they have no known competing financial interests or personal relationships that could have appeared to influence the work reported in this paper.

Data availability

Sequence data were deposited at the Sequence Read Archive (SRA, NCBI) under Bioproject PRJNA892267

Acknowledgments

This work was supported by the grant “Sviluppo Catalisi dell’Innovazione nelle Biotecnologie” (MIUR ex D.M.738 dd 08/08/19) of the Consorzio Interuniversitario per le Biotecnologie (CIB) and by the China Scholarship Council (No. 202008310162).

Appendix A. Supplementary data

Supplementary data to this article can be found online at https://doi.org/10.1016/j.cej.2023.143589.

References

[1] C. Luís, M. Algarra, J.S. Câmara, R. Perestrelo, Comprehensive insight from phthalates occurrence: from health outcomes to emerging analytical approaches, Toxics 9 (2021) 157.
[2] Y. Ma, S. Liao, Q. Li, Q. Guan, P. Jia, Y. Zhou, Physical and chemical modifications of poly (vinyl chloride) materials to prevent plasticizer migration-Still on the run, React. Funct. Polym. 147 (2020), 104458.
[3] P. Chakraborty, N.W. Shappell, M. Mukhopadhyay, S. Onanong, K.R. Rex, D. Snow, Surveillance of plasticizers, bisphenol A, steroids and caffeine in surface water of river Ganga and Sundarban wetland along the Bay of Bengal: occurrence, sources, estrogenicity screening and ecotoxicological risk assessment, Water Res. 190 (2021), 116668.
[4] M. Zhou, J. Yang, Y. Li, A model for phthalic acid esters’ biodegradability and biotoxicity multi-effect pharmacophore and its application in molecular modification, J. Environ. Sci. Health A 56 (2021) 361–378.
[5] X. Zhang, L. He, A.K. Sarmah, K. Lin, Y. Liu, J. Li, H. Wang, Retention and release of diethyl phthalate in biochar-amended vegetable garden soils, J. Soil. Sediment. 14 (11) (2014) 1790–1799.
[6] R. Jamarani, H.C. Erythropel, J.A. Nicell, R.L. Leask, M. Marić, How green is your plasticizer? Polymers 10 (2018) 834.
[7] J. Kastner, D.G. Cooper, M. Marić, P. Dodd, V. Yargeau, Aqueous leaching of di-2-ethylhexyl phthalate and “green” plasticizers from poly vinyl chloride, Sci. Total Environ. 432 (2012) 357–364.
[8] C.M. Chan, R. Lyons, P.G. Dennis, P. Lant, S. Pratt, B. Laycock, Effect of toxic phthalate-based plasticizer on the biodegradability of polyhydroxyalkanoate, Environ. Sci. Tech. 56 (24) (2022) 17732–17742.
[9] L. Xu, W. Chu, L. Gan, Environmental application of graphene-based CoFe2O4 as an activator of peroxymonosulfate for the degradation of a plasticizer, Chem. Eng. J. 263 (2015) 435–443.
[10] A. Kumari, R. Kaur, Uptake of a plasticizer (di-n-butyl phthalate) impacts the biochemical and physiological responses of barley, PeerJ 10 (2022) e12859.
[11] J.A. Pedersen, M. Soliman, I.H.(. Suffet, Human pharmaceuticals, hormones, and personal care product ingredients in runoff from agricultural fields irrigated with treated wastewater, J. Agric. Food Chem. 53 (5) (2005) 1625–1632.
[12] R.T. Lumio, M.A. Tan, H.D. Magpantay, Biotechnology-based microbial degradation of plastic additives, 3, Biotech 11 (2021) 350.
[13] M.W. Lim, E.V. Lau, P.E. Poh, A comprehensive guide of remediation technologies for oil contaminated soil—present works and future directions, Mar. Pollut. Bull. 109 (1) (2016) 14–45.
[14] S. Bala, D. Garg, B.V. Thirumalesh, M. Sharma, K. Sridhar, B.S. Inbaraj, M. Tripathi, Recent strategies for bioremediation of emerging pollutants: a review for a green and sustainable environment, Toxics 10 (2022) 484.
[15] S. Shariati, A.A. Pourbabaee, H.A. Alikhani, Biodegradation of diethyl phthalate and phthalic acid by a new indigenous Pseudomonas putida, Folia Microbiol. (2023) 1–12.
[16] Z.-D. Wen, D.-W. Gao, W.-M. Wu, Biodegradation and kinetic analysis of phthalates by an Arthrobacter strain isolated from constructed wetland soil, Appl. Microbiol. Biotechnol. 98 (10) (2014) 4683–4690.
[17] M. Boll, R. Geiger, M. Junghare, B. Schink, Microbial degradation of phthalates: biochemistry and environmental implications, Environ. Microbiol. Rep. 12 (1) (2020) 3–15.
[18] Y. Wang, Q. Ren, W. Zhan, K. Zheng, Q.i. Liao, Z. Yang, Y. Wang, X. Ruan, Biodegradation of di-n-octyl phthalate by Gordonia sp Lff and its application in soil, Environmental Technology 43 (17) (2022) 2604–2611.
[19] W. Jianlong, Z. Xuan, W.u. Weizhong, Biodegradation of phthalic acid esters (PAEs) in soil bioaugmented with acclimated activated sludge, Process Biochem. 39 (12) (2004) 1837–1841.
[20] Y. Xie, H. Liu, H. Li, H. Tang, H. Peng, H. Xu, High-effectively degrade the di-(2-ethylhexyl) phthalate via biochemical system: Resistant bacterial flora and persulfate oxidation activated by BC@ Fe3O4, Environ. Pollut. 262 (2020), 114100.
[21] M. Ji, X. Wang, M. Usman, F. Liu, Y. Dan, L. Zhou, S. Campanaro, G. Luo, W. Sang, Effects of different feedstocks-based biochar on soil remediation: a review, Environ. Pollut. 294 (2022) 118655.
[22] C. Zhang, G. Zeng, D. Huang, C. Lai, M. Chen, M. Cheng, W. Tang, L. Tang, H. Dong, B. Huang, Biochar for environmental management: Mitigating greenhouse gas emissions, contaminant treatment, and potential negative impacts, Chem. Eng. J. 373 (2019) 902–922.
[23] Y. Yi, Z. Huang, B. Lu, J. Xian, E.P. Tsang, W. Cheng, J. Fang, Z. Fang, Magnetic biochar for environmental remediation: A review, Bioresour. Technol. 298 (2020) 122468.
[24] A.R. Zimmerman, B. Gao, M.-Y. Ahn, Positive and negative carbon mineralization priming effects among a variety of biochar-amended soils, Soil Biol. Biochem. 43 (6) (2011) 1169–1179.
[25] X. Zhang, A.K. Sarmah, N.S. Bolan, L. He, X. Lin, L. Che, C. Tang, H. Wang, Effect of aging process on adsorption of diethyl phthalate in soils amended with bamboo biochar, Chemosphere 142 (2016) 28–34.
[26] M. Ji, W. Sang, D.C. Tsang, M. Usman, S. Zhang, G. Luo, Molecular and microbial insights towards understanding the effects of hydrochar on methane emission from paddy soil, Sci. Total Environ. 714 (2020), 136769.
[27] I. Koo, X. Zhang, S. Kim, Wavelet-and Fourier-transform-based spectrum similarity approaches to compound identification in gas chromatography/mass spectrometry, Anal. Chem. 83 (14) (2011) 5631–5638.
[28] A. Chklovski, D.H. Parks, B.J. Woodcroft, G.W. Tyson, CheckM2: a rapid, scalable and accurate tool for assessing microbial genome quality using machine learning, bioRxiv (2022) 2022.2007. 2011.499243.
[29] C. Piñeiro, J.M. Abuín, J.C. Pichel, Very Fast Tree: speeding up the estimation of phylogenies for large alignments through parallelization and vectorization strategies, Bioinformatics 36 (2020) 4658–4659.
[30] J. Hadfield, N.J. Croucher, R.J. Goater, K. Abudahab, D.M. Aanensen, S.R. Harris, Phandango: an interactive viewer for bacterial population genomics, Bioinformatics 34 (2018) 292–293.
[31] B.P. Alcock, A.R. Raphenya, T.T.Y. Lau, K.K. Tsang, M. Bouchard, A. Edalatmand, W. Huynh, A.-L. Nguyen, A.A. Cheng, S. Liu, S.Y. Min, A. Miroshnichenko, H.-K. Tran, R.E. Werfalli, J.A. Nasir, M. Oloni, D.J. Speicher, A. Florescu, B. Singh, M. Faltyn, A. Hernandez-Koutoucheva, A.N. Sharma, E. Bordeleau, A. C. Pawlowski, H.L. Zubyk, D. Dooley, E. Griffiths, F. Maguire, G.L. Winsor, R. G. Beiko, F.S.L. Brinkman, W.W.L. Hsiao, G.V. Domselaar, A.G. McArthur, antibiotic resistome surveillance with the comprehensive antibiotic resistance database, Nucleic Acids Res. (2020).
[32] B. Liu, D. Zheng, Q. Jin, L. Chen, J. Yang, VFDB 2019: a comparative pathogenomic platform with an interactive web interface, Nucleic Acids Res. 47 (2019) (2019) D687–D692.
[33] M. Xi, K. Cui, M. Cui, Y. Ding, Z. Guo, Y. Chen, C. Li, X. Li, Enhanced norfloxacin degradation by iron and nitrogen co-doped biochar: revealing the radical and nonradical co-dominant mechanism of persulfate activation, Chem. Eng. J. 420 (2021), 129902.
[34] S. Hao, X. Zhu, Y. Liu, F. Qian, Z. Fang, Q. Shi, S. Zhang, J. Chen, Z.J. Ren, Production temperature effects on the structure of hydrochar-derived dissolved organic matter and associated toxicity, Environ. Sci. Tech. 52 (13) (2018) 7486–7495.
[35] J.A. Korak, E.C. Wert, F.L. Rosario-Ortiz, Evaluating fluorescence spectroscopy as a tool to characterize cyanobacteria intracellular organic matter upon simulated release and oxidation in natural water, Water Res. 68 (2015) 432–443.
[36] R. Guo, L. Yan, P. Rao, R. Wang, X. Guo, Nitrogen and sulfur co-doped biochar derived from peanut shell with enhanced adsorption capacity for diethyl phthalate, Environ. Pollut. 258 (2020), 113674.
[37] J. Yan, G. Quan, Sorption behavior of dimethyl phthalate in biochar-soil composites: implications for the transport of phthalate esters in long-term biochar amended soils, Ecotoxicol. Environ. Saf. 205 (2020), 111169.
[38] C.-D. Dong, C.-W. Chen, C.-M. Hung, Persulfate activation with rice husk-based magnetic biochar for degrading PAEs in marine sediments, Environ. Sci. Pollut. Res. 26 (33) (2019) 33781–33790.
[39] W.J. Adams, G.R. Biddinger, K.A. Robillard, J.W. Gorsuch, A summary of the acute toxicity of 14 phthalate esters to representative aquatic organisms, Environmental Toxicology and Chemistry: an Int. J. 14 (1995) 1569–1574.
[40] J. Gao, Z. Shi, H. Wu, J. Lv, Fluorescent characteristics of dissolved organic matter released from biochar and paddy soil incorporated with biochar, RSC Adv. 10 (10) (2020) 5785–5793.
[41] Y. Yamashita, E. Tanoue, Chemical characterization of protein-like fluorophores in DOM in relation to aromatic amino acids, Mar. Chem. 82 (3-4) (2003) 255–271.
[42] C.J. Williams, Y. Yamashita, H.F. Wilson, R. Jaffé, M.A. Xenopoulos, Unraveling the role of land use and microbial activity in shaping dissolved organic matter characteristics in stream ecosystems, Limnol. Oceanogr. 55 (3) (2010) 1159–1171.

[43] P.G. Coble, Marine optical biogeochemistry: the chemistry of ocean color, Chem. Rev. 107 (2007) 402–418.
[44] N. Ferretto, M. Tedetti, C. Guigue, S. Mounier, R. Redon, M. Goutx, Identification and quantification of known polycyclic aromatic hydrocarbons and pesticides in complex mixtures using fluorescence excitation–emission matrices and parallel factor analysis, Chemosphere 107 (2014) 344–353.
[45] J. Šerá, F. Huynh, F. Ly, Š. Vinter, M. Kadlečková, V. Krátká, D. Máčalová, M. Koutný, C. Wallis, Biodegradable polyesters and low molecular weight polyethylene in soil: interrelations of material properties, Soil Organic Matter Substances, and Microbial Community, International Journal of Molecular Sciences 23 (2022) 15976.
[46] B. Aftab, H.-S. Shin, J. Hur, Exploring the fate and oxidation behaviors of different organic constituents in landfill leachate upon Fenton oxidation processes using EEM-PARAFAC and 2D-COS-FTIR, J. Hazard. Mater. 354 (2018) 33–41.
[47] K. Li, W. Jia, L. Xu, M. Zhang, Y. Huang, The plastisphere of biodegradable and conventional microplastics from residues exhibit distinct microbial structure, network and function in plastic-mulching farmland, J. Hazard. Mater. 442 (2023), 130011.
[48] P.V. Gavande, A. Basak, S. Sen, K. Lepcha, N. Murmu, V. Rai, D. Mazumdar, S. P. Saha, V. Das, S. Ghosh, Functional characterization of thermotolerant microbial consortium for lignocellulolytic enzymes with central role of Firmicutes in rice straw depolymerization, Sci. Rep. 11 (2021) 1–13.
[49] M.N. Fawaz, Revealing the ecological role of Gemmatimonadetes through cultivation and molecular analysis of agricultural soils, (2013).
[50] P.H. Janssen, P.S. Yates, B.E. Grinton, P.M. Taylor, M. Sait, Improved culturability of soil bacteria and isolation in pure culture of novel members of the divisions Acidobacteria, Actinobacteria, Proteobacteria, and Verrucomicrobia, Appl. Environ. Microbiol. 68 (5) (2002) 2391–2396.
[51] N. Ren, Y. Wang, Y. Ye, Y. Zhao, Y. Huang, W. Fu, X. Chu, Effects of continuous nitrogen fertilizer application on the diversity and composition of rhizosphere soil bacteria, Front. Microbiol. 11 (2020) 1948.
[52] M. Hernández, P. Villalobos, V. Morgante, M. González, C. Reiff, E. Moore, M. Seeger, Isolation and characterization of a novel simazine-degrading bacterium from agricultural soil of central Chile, Pseudomonas sp. MHP41, FEMS microbiology letters 286 (2008) 184-190.
[53] M.A. Pereyra-Camacho, V.E. Balderas-Hernández, A. De Leon-Rodriguez, Biodegradation of diisononyl phthalate by a consortium of saline soil bacteria: optimisation and kinetic characterisation, Appl. Microbiol. Biotechnol. 105 (8) (2021) 3369–3380.
[54] S.-G. Woo, Y. Cui, M.-S. Kang, L. Jin, K.K. Kim, S.-T. Lee, M. Lee, J. Park, Georgenia daeguensis sp. nov., isolated from 4-chlorophenol enrichment culture, Int. J. Syst. Evol. Microbiol. 62 (2012) 1703–1709.
[55] Y. Wang, H. Liu, Y. Peng, L. Tong, L. Feng, K. Ma, New pathways for the biodegradation of diethyl phthalate by Sphingobium yanoikuyae SHJ, Process Biochem. 71 (2018) 152–158.
[56] X. Zhang, R. Li, J. Song, Y. Ren, X.i. Luo, Y.i. Li, X. Li, T. Li, X. Wang, Q. Zhou, Combined phyto-microbial-electrochemical system enhanced the removal of petroleum hydrocarbons from soil: a profundity remediation strategy, J. Hazard. Mater. 420 (2021) 126592.
[57] C. Dai, H. Wu, X. Wang, K. Zhao, Z. Lu, Network and meta-omics reveal the cooperation patterns and mechanisms in an efficient 1, 4-dioxane-degrading microbial consortium, Chemosphere 301 (2022), 134723.
[58] Y. Teng, X. Wang, L. Li, Z. Li, Y. Luo, Rhizobia and their bio-partners as novel drivers for functional remediation in contaminated soils, Front. Plant Sci. 6 (2015) 32.
[59] C. Pagnout, G. Frache, P. Poupin, B. Maunit, J.-F. Muller, J.-F. Férard, Isolation and characterization of a gene cluster involved in PAH degradation in Mycobacterium sp. strain SNP11: Expression in Mycobacterium smegmatis mc2155, Res. Microbiol. 158 (2007) 175–186.
[60] D.-W. Liang, T. Zhang, H.H. Fang, J. He, Phthalates biodegradation in the environment, Appl. Microbiol. Biotechnol. 80 (2008) 183–198.
[61] G. Wang, W. Yue, Y. Liu, F. Li, M. Xiong, H. Zhang, Biodegradation of the neonicotinoid insecticide Acetamiprid by bacterium Pigmentiphaga sp. strain AAP-1 isolated from soil, Bioresour. Technol. 138 (2013) 359–368.
[62] H. Yang, X. Wang, J. Zheng, G. Wang, Q. Hong, S. Li, R. Li, J. Jiang, Biodegradation of acetamiprid by Pigmentiphaga sp. D-2 and the degradation pathway, International Biodeterioration & Biodegradation 85 (2013) 95-102.
[63] H. Yu, L. Wang, Y. Lin, W. Liu, D. Tuyiringire, Y. Jiao, L. Zhang, Q. Meng, Y. Zhang, Complete metabolic study by dibutyl phthalate degrading Pseudomonas sp. DNB-S1, Ecotoxicol. Environ. Saf. 194 (2020), 110378.
[64] P. Cornelis, Iron uptake and metabolism in pseudomonads, Appl. Microbiol. Biotechnol. 86 (6) (2010) 1637–1645.
[65] C. Gómez-Garzón, J.E. Barrick, S.M. Payne, E.G. Ruby, Disentangling the evolutionary history of Feo, the major ferrous iron transport system in bacteria, MBio 13 (1) (2022).
[66] H. Kim, H. Lee, D. Shin, The FeoA protein is necessary for the FeoB transporter to import ferrous iron, Biochem. Biophys. Res. Commun. 423 (4) (2012) 733–738.
[67] F. Hoegy, H. Celia, G.L. Mislin, M. Vincent, J. Gallay, I.J. Schalk, Binding of iron-free siderophore, a common feature of siderophore outer membrane transporters of Escherichia coli and Pseudomonas aeruginosa, J. Biol. Chem. 280 (21) (2005) 20222–20230.
[68] R. Hu, H. Zhao, X. Xu, Z. Wang, K. Yu, L. Shu, Q. Yan, B. Wu, C. Mo, Z. He, Bacteria-driven phthalic acid ester biodegradation: Current status and emerging opportunities, Environ. Int. 154 (2021), 106560.
[69] L. Niu, W. Liu, A. Juhasz, J. Chen, L. Ma, Emerging contaminants antibiotic resistance genes and microplastics in the environment: Introduction to 21 review articles published in CREST during 2018–2022, Crit. Rev. Environ. Sci. Technol. 52 (2022) 4135–4146.
[70] D. Zhu, J. Ma, G. Li, M.C. Rillig, Y.-G. Zhu, Soil plastispheres as hotspots of antibiotic resistance genes and potential pathogens, ISME J. 16 (2) (2022) 521–532.
[71] M. Hernandez, S. Roy, C.W. Keevil, M.G. Dumont, Identification of diverse antibiotic resistant bacteria in agricultural soil with H218O stable isotope probing and metagenomics, bioRxiv (2023) 2023.2001. 2024.525391.
[72] H. Liao, H. Li, C.-S. Duan, X.-Y. Zhou, X.-L. An, Y.-G. Zhu, J.-Q. Su, Metagenomic and viromic analysis reveal the anthropogenic impacts on the plasmid and phage borne transferable resistome in soil, Environ. Int. 170 (2022), 107595.
[73] A.S. Cross, What is a virulence factor? Crit. Care 12 (2008) 1–2.
[74] L.L. Burrows, Pseudomonas aeruginosa twitching motility: type IV pili in action, Annu. Rev. Microbiol. 66 (1) (2012) 493–520.
[75] G. Ghssein, Z. Ezzeddine, A review of Pseudomonas aeruginosa metallophores: Pyoverdine, pyochelin and pseudopaline, Biology 11 (2022) 1711.
[76] M. Michalska, P. Wolf, Pseudomonas Exotoxin A: optimized by evolution for effective killing, Front. Microbiol. 6 (2015) 963.